Direct writing of ferroelectric domains on strontium barium niobate crystals using focused ultraviolet laser light

Andreas Boes,[1,a)] Tristan Crasto,[1] Hendrik Steigerwald,[1] Scott Wade,[2] Jakob Frohnhaus,[3] Elisabeth Soergel,[3] and Arnan Mitchell[1]
[1]*School of Electrical and Computer Engineering and ARC Center for Ultra-High Bandwidth Devices for Optical Systems (CUDOS), RMIT University, Melbourne, Victoria 3001, Australia*
[2]*Faculty of Engineering and Industrial Sciences, Swinburne University of Technology, Hawthorn, Victoria 3122, Australia*
[3]*Institute of Physics, University of Bonn, Wegelerstr. 8, 53115 Bonn, Germany*

(Received 15 April 2013; accepted 14 September 2013; published online 30 September 2013)

We report ferroelectric domain inversion in strontium barium niobate (SBN) single crystals by irradiating the surface locally with a strongly focused ultraviolet (UV) laser beam. The generated domains are investigated using piezoresponse force microscopy. We propose a simple model that allows predicting the domain width as a function of the irradiation intensity, which indeed applies for both SBN and $LiNbO_3$. Evidently, though fundamentally different, the domain structure of both SBN and $LiNbO_3$ can be engineered through similar UV irradiation. © *2013 AIP Publishing LLC*. [http://dx.doi.org/10.1063/1.4823702]

Ferroelectric crystals are widely used for nonlinear optical applications, such as frequency conversion employing quasi-phase matching, which requires periodic poling of the crystal. Strontium barium niobate ($Sr_xBa_{1-x}Nb_2O_6$, SBN) has become an encouraging material for optical applications,[1–3] due to its excellent electro-optic,[4] acousto-optic,[5] and nonlinear-optical properties.[6] Accordingly, domain engineering in SBN is an active field of research.

It has already been shown in the 1970s that temperature gradients can be used to determine the spontaneous polarization in lithium niobate ($LiNbO_3$).[7,8] Very recently, domain patterns were controllably generated on all crystal faces of $LiNbO_3$ by scanning a strongly focused, highly absorbed ultraviolet (UV) laser beam across the surface.[9,10] The proposed domain inversion mechanism of this technique by Steigerwald *et al.*[10] is also based on temperature gradients and reads as follows: UV laser light induces a high temperature, localized at the crystal's surface, due to the strong absorption of UV light. The resulting temperature gradient can reach values as large as $>200\,K/\mu m$. This strong temperature gradient induces an electric field of thermoelectric origin. The induced electric field can exceed the coercive field of the crystal, thus defining (and thus possibly also inverting) the direction of spontaneous polarization. The advantage of this domain engineering method is not only the independence of the domain patterns on the crystallographically preferred directions, but it can also be applied in situations where electric field poling cannot be used as, for instance, when processing *x*-cut $LiNbO_3$ crystals.[10]

Thus far, the technique of UV laser-induced domain formation has only been reported for $LiNbO_3$. In principle, however, it should be equally applicable to any ferroelectric crystal. In this contribution, we show that ferroelectric domain inversion by focused UV laser light can also be used for materials other than $LiNbO_3$, namely, the relaxor ferroelectric SBN.

UV laser-induced domain formation owing to the thermoelectric effect was shown for the non-polar faces of $LiNbO_3$.[10] However, in this contribution, *c*-cut SBN crystals are utilized. This requires the transformation of the above-mentioned process to the polar faces as it is illustrated qualitatively in Fig. 1. In (a), the temperature profile along the polar *c*-axis is shown, and in (b), the resulting temperature gradient is depicted. The electric field, which is induced by the temperature gradient ($E = Q_{33}dT/dc$), is shown in (c). Figs. 1(a)–1(c) illustrate the thermoelectric behavior on the $+c$ face, and (d) to (f) on the $-c$ face. As it can be seen from Fig. 1, domain inversion by the thermoelectric effect is basically only possible on the $-c$ face of the crystal (which is in accordance with the findings from Muir *et al.*[12] on $LiNbO_3$). If the UV-induced temperature is below the Curie temperature (Fig. 1(f)), it is the interplay of the strength of the thermoelectric field and the coercive field, which defines the depth and width of the generated domain. If the UV-induced temperature is above the Curie temperature, there is by definition no coercive field, and the thermoelectric field possibly generates tail-to-tail domains. This is especially interesting for SBN, which has a Curie temperature of $T_C = 343\,K$ only.[1]

Taking the mechanism explained above, we propose the following model to predict the domain width as a function of UV irradiation intensity: The temperature profile, which is induced on the crystal surface (along the *x*- and *y*-axis) by the focused UV laser beam, follows approximately a Gaussian function,[11] resulting in a temperature gradient profile, which also follows the same function. For obtaining the domain width as a function of the UV laser light intensity, we assume that the intensity, and therefore the induced temperature gradient, must exceed a certain threshold before domain inversion is achieved (as it has also been observed on $LiNbO_3$ by Muir *et al.*[12]). The exact value of the intensity threshold depends on several material parameters (listed in Table I), which govern the domain inversion process.[10]

To support the threshold assumption an illustration is given in Fig. 2, where (a), (b), and (c) are Gaussian functions

a)Electronic mail: s3363819@student.rmit.edu.au

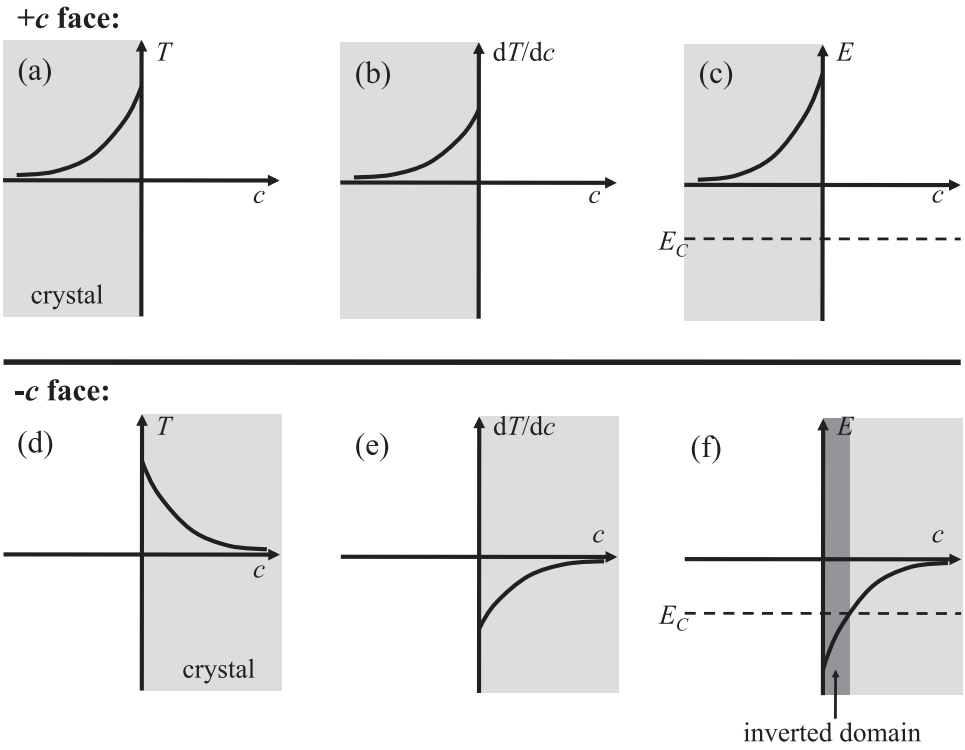

FIG. 1. Illustration of the induced thermoelectric field (all axes in arbitrary units). (a) The temperature profile along the polar *c*-axis, resulting in a temperature gradient, which is shown in (b). (c) The electric field, which is induced due to the temperature gradient. (a)–(c) The thermoelectric behavior on the $+c$ face, whereas (d)–(f) show this on the $-c$ face.

each with a maxima of −1.0, −0.7, and −0.4 arbitrary units. The horizontal lines illustrate assumed temperature gradient thresholds of $LiNbO_3$ and SBN, respectively. Consequently the intersections of the curves (a), (b), and (c) with these thresholds would define the width of the inverted domains for the corresponding crystal. Given a typical Gaussian function $f = I\exp(-d^2/2g^2)$, if this is solved for d, then the dependence of the domain width d from the temperature gradient, respectively, the UV laser light intensity I can be expressed as

$$d = \sqrt{-2g^2\ln(f/I)}, \tag{1}$$

where g determines the width of the Gaussian function and f determines the threshold.

For our experimental investigations, a 1-mm-thick, *c*-cut crystal of congruent SBN ($Sr_{0.61}Ba_{0.39}Nb_2O_6$) from "Oxide Corporation" was investigated. A frequency-doubled argon ion laser provided continuous wave UV light with a wavelength of 244 nm. The UV laser light was focused onto the surface of the crystals by a lens with a focal length of 40 mm. The focal width of the beam was approximately 7 μm. A three-axis computer-controlled translation stage was used for scanning the sample, tracking with a velocity of 0.1 mm/s. The writing intensity was varied from 1.5×10^5 to 3.6×10^5 W/cm^2. The written domain patterns were investigated by piezoresponse force microscopy (PFM).[13]

For comparison, we also investigated a 0.5-mm-thick *c*-cut crystal of congruent $LiNbO_3$ from "Crystal Technology." The domain patterns on this crystal were investigated both by PFM and by HF etching.

The experimental results for SBN are presented in Fig. 3, where (a) and (b) show PFM images of the domains written on the $-c$ face of the crystal with different writing intensities. The three bright stripes seen in the two PFM images correspond to the inverted UV-written domains. The writing intensities were $I = 2.9\times10^5$ and 2.3×10^5 W/cm^2, which resulted in domain widths of approximately 17.2 ± 0.5 and 13.7 ± 0.7 μm, for (a) and (b), respectively. The given domain widths are the average of the width of three UV-written domain tracks. The result of UV laser irradiation ($I = 2.3\times10^5$ W/cm^2) on the $+c$ face of the SBN crystal is shown in Fig. 3(c). The dark circular patterns are $-c$ oriented areas, which were present in some areas of the

TABLE I. Comparison between the coefficients, which influence the UV direct domain writing technique for SBN and $LiNbO_3$. Unfortunately, the thermoelectric power value Q_{33} along the *c*-axis, which generates an electric field in the crystal due to the temperature gradient, could not be found in the literature for congruent SBN.

	$LiNbO_3$	SBN
Absorption α (at 244 nm)	3×10^7 1/m (Ref. 15)	4.8×10^7 1/m (Ref. 16)
Reflectivity R (at 244 nm)	0.27 (Ref. 15)	0.27 (Ref. 16)
Thermal diffusivity D	14×10^{-3} cm^2/s (Ref. 19)	6.8×10^{-3} cm^2/s (Ref. 20)
Coercive field E_c	21 kV/mm	1.3 kV/mm (Ref. 1)
Curie temperature T_C	1415 K	343 K (Ref. 1)
Melting temperature T_m	1530 K	1765 K (Ref. 21)
Thermoelectric power Q_{33} (at T_C)	0.8 mV/K (Ref. 8)	…

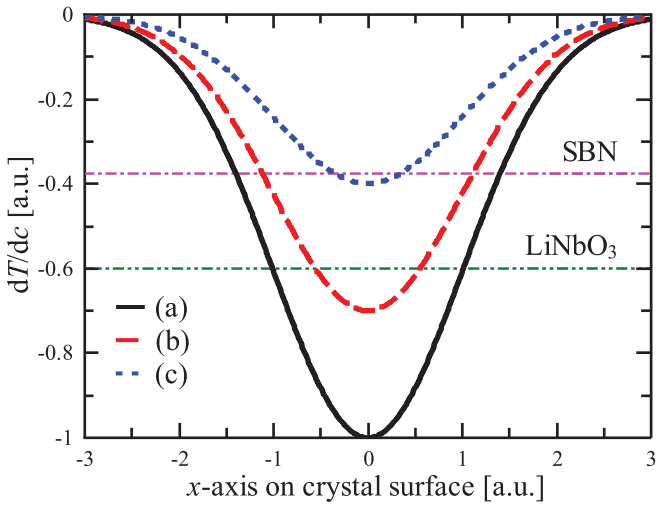

FIG. 2. Illustration of the assumed threshold behavior. (a)–(c) are Gaussian functions with maxima of −1.0, −0.7, and −0.4, respectively. The horizontal lines illustrate the temperature gradient thresholds of $LiNbO_3$ and SBN. The intersections of (a), (b), and (c) with the thresholds would then define the width of the inverted domain for the corresponding crystal.

crystal before the UV irradiating process and is shown in Fig. 4. Indeed, it can be seen that the UV-written tracks invert only the $-c$ oriented areas, whereas the $+c$ oriented areas do not change their polarization. The depth resolution of the PFM in $LiNbO_3$ is $\sim 1.7\ \mu m$;[14] based on this, we estimate the depth of the UV written domains in SBN to be deeper than this value.

Figure 5 depicts the dependence of the domain width as a function of the writing intensity for both SBN and $LiNbO_3$. The graph furthermore shows that domains in SBN can be inverted by lower laser intensities compared to $LiNbO_3$ and finally that the domains in SBN are, in general, wider than

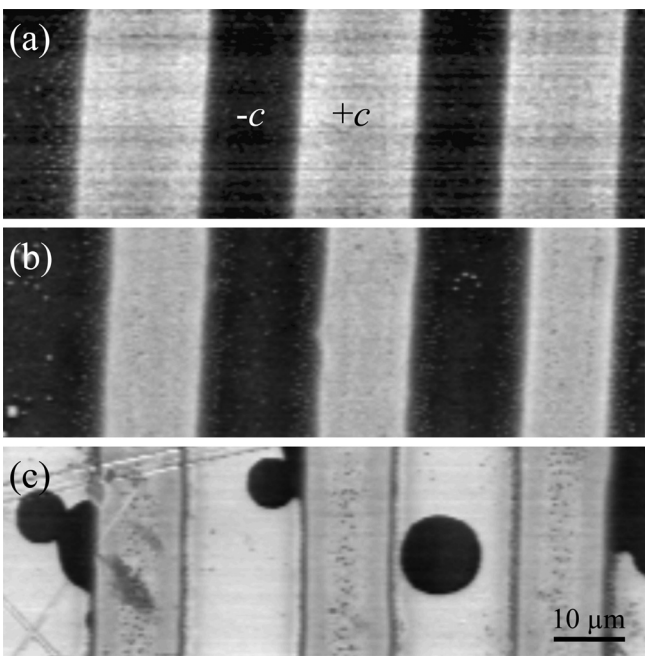

FIG. 3. PFM pictures of UV-written tracks on the SBN crystal. (a) and (b) show domain inverted areas (three bright stripes) by UV irradiation on the $-c$ face with an intensity of 2.9×10^5 and $2.3 \times 10^5\ W/cm^2$, respectively. (c) UV-written tracks ($I = 2.3 \times 10^5\ W/cm^2$) on the $+c$ face, where the tracks do not invert the crystal polarization.

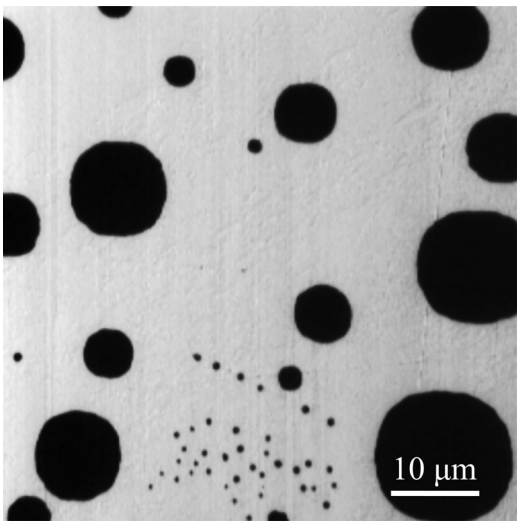

FIG. 4. PFM image of the SBN crystal's initial domain state on the $-c$ face.

those in $LiNbO_3$. The result from our simple model (Eq. (1)) is also plotted in Fig. 5, whereby the parameters g and f were chosen to best fit the experimental data. Evidently, our model describes the experimental results well (R^2 is 0.998 and 0.983 for fitted functions of SBN and $LiNbO_3$, respectively). From the graphs, one can now read the threshold for achieving domain inversion, which is given by the intersection of the fitting function with the x-axis, which is $1.47 \times 10^5\ W/cm^2$ for SBN and $2.53 \times 10^5\ W/cm^2$ for $LiNbO_3$.

The fact that for both crystals, SBN and $LiNbO_3$, direct writing of domains is only possible on the $-c$ face of the crystal,[9,12] and that the same model can be utilized to fit the experimental data, suggests that the physical mechanism used to explain domain generation in $LiNbO_3$ (Ref. 10) is also applicable to SBN. This is on the one hand surprising, as the material parameters, which govern UV-induced direct writing of domains, differ substantially for SBN and for $LiNbO_3$ (Table I). On the other hand, their difference can help to explain the different behavior of the two crystals regarding UV laser-induced direct writing of domains. The reflectivity R of the two crystals being identical, the same

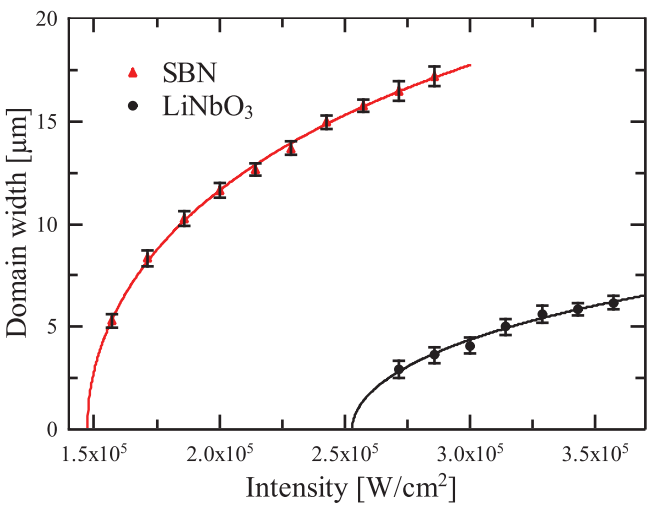

FIG. 5. Measured domain width on the SBN and $LiNbO_3$ crystals as a function of the UV laser light intensity. Equation (1) was used for fitting the experimental measured data points.

amount of UV laser light enters both crystals. Same than in $LiNbO_3$, the UV laser light entering the SBN crystal is absorbed at the very surface (<100 nm). The twice as large thermal diffusivity of $LiNbO_3$, compared to SBN, leads to a wider temperature profile in $LiNbO_3$. The values so far suggest that the written domains should be wider in $LiNbO_3$ than in SBN. However, both the coercive field and the Curie temperature are substantially lower for SBN when compared to $LiNbO_3$. These significant differences could explain why a lower UV laser light intensity is needed to reach the threshold for domain inversion in SBN. This behavior is also reflected in Fig. 5 where domains on SBN are written at much lower intensities compared to $LiNbO_3$. The low-intensity threshold for SBN together with the higher melting temperature of SBN has a positive side-effect, namely, the problem of UV laser-induced surface damage during direct writing of domains, as is present in $LiNbO_3$,[12] was not observed in SBN.

The domain inversion model by Steigerwald *et al.*,[10] which was used to discuss the results, is mainly based on the thermoelectric field that is induced due to the strong temperature gradient. However, also other effects, which have an impact on domain inversion, might take place during heating and cooling of ferroelectric crystals. Especially bulk screening effects have to be considered, which are a result of the increased conductivity and the pyroelectric effect.[17,18] Also, the diffuse phase transition and the formation of domain structures in relaxors (SBN) are quite different from normal ferroelectric crystals ($LiNbO_3$), which can further influence the domain inversion process. Full understanding of the domain inversion process by UV laser direct writing not only in SBN, but also in $LiNbO_3$, does certainly require further investigations. For practical applications, however, the proposed model allows to predict the generated domain width based on the UV-laser intensity.

In summary, we have experimentally demonstrated that the UV direct domain writing technique works not only on lithium niobate, but also on strontium barium niobate. Furthermore, we have gained deeper insight into the UV domain writing process by a better understanding of the crucial role the thermoelectric effect, the Curie temperature, and coercive field strength of the ferroelectric material plays. These results suggest that the UV domain writing technique can also be applied for other ferroelectric crystals.

The authors acknowledge the facilities, and the scientific and technical assistance of the Australian Microscopy & Microanalysis Research Facility at RMIT University and the Faculty of Engineering and Industrial Sciences at Swinburne University of Technology. This work was made possible through the generous support of CUDOS.

[1]Y. Y. Zhu, J. S. Fu, R. F. Xiao, and G. K. L. Wong, Appl. Phys. Lett. **70**, 1793 (1997).
[2]D. Jaque, N. D. Psaila, R. R. Thomson, F. Chen, L. M. Maestro, A. Ródenas, D. T. Reid, and A. K. Kar, Appl. Phys. Lett. **96**, 191104 (2010).
[3]Y. Tan, F. Chen, and H.-J. Zhang, Opt. Express **15**, 16696–16701 (2007).
[4]P. V. Lenzo, Appl. Phys. Lett. **11**, 23 (1967).
[5]R. R. Neurgaonkar, W. K. Cory, W. W. Ho, W. F. Hall, and L. E. Cross, Ferroelectrics **38**, 857–860 (1981).
[6]M. Horowitz, A. Bekker, and B. Fischer, Appl. Phys. Lett. **62**, 2619 (1993).
[7]M. Tasson, H. Legal, J. C. Gay, J. C. Peuzin, and F. C. Lissalde, Ferroelectrics **13**, 479 (1976).
[8]Y. S. Luh, R. S. Feigelson, M. M. Fejer, and R. L. Byer, J. Cryst. Growth **78**, 135–143 (1986).
[9]C. Y. J. Ying, A. C. Muir, C. E. Valdivia, H. Steigerwald, C. L. Sones, R. W. Eason, E. Soergel, and S. Mailis, Laser Photonics Rev. **6**, 526–548 (2012).
[10]H. Steigerwald, Y. J. Ying, R. W. Eason, K. Buse, S. Mailis, and E. Soergel, Appl. Phys. Lett. **98**, 062902 (2011).
[11]A. C. Muir, G. J. Daniell, C. P. Please, I. T. Wellington, S. Mailis, and R. W. Eason, Appl. Phys. A **83**, 389–396 (2006).
[12]A. C. Muir, C. L. Sones, S. Mailis, R. W. Eason, T. Jungk, A. Hoffman, and E. Soergel, Opt. Express **16**, 2336–2350 (2008).
[13]E. Soergel, J. Phys. D **44**, 464003 (2011).
[14]F. Johann, Y. J. Ying, T. Jungk, A. Hoffmann, C. L. Sones, R. W. Eason, S. Mailis, and E. Soergel, Appl. Phys. Lett. **94**, 172904 (2009).
[15]A. M. Mamedov, Opt. Spectrosc. **56**, 645 (1984).
[16]K. Dorywalski, B. Andriyevsky, C. Cobet, M. Piasecki, I. V. Kityk, N. Esser, T. Łukasiewicz, and A. Patryn, Opt. Mater. **35**, 887 (2013).
[17]V. Y. Shur, D. K. Kuznetsov, E. A. Mingaliev, E. M. Yakunina, A. I. Lobov, and A. V. Ievlev, Appl. Phys. Lett. **99**, 082901 (2011).
[18]A. I. Lobov, V. Y. Shur, D. K. Kuznetsov, S. A. Negashev, D. V. Pelegov, E. I. Shishkin, and P. S. Zelenovskiy, Ferroelectrics **373**, 99 (2008).
[19]C. L. Choy, W. P. Leung, T. G. Xi, Y. Fei, and C. F. Shao, J. Appl. Phys. **71**, 170 (1992).
[20]R. A. Morgan, K. I. Kang, C. C. Hsu, C. L. Koliopoulos, and N. Peyghambarian, Appl. Opt. **26**, 5266–5271 (1987).
[21]M. Ulex, R. Pankrath, and K. Betzler, J. Cryst. Growth **271**, 128–133 (2004).